

# Digital Twin-Based Modeling of an Electric Vessel Fast Charger for Cloud Implementation

Gorka Elezgarai  
Department of Energy Storage  
and Power Electronics (BPE)  
Ikerlan Technology Research  
Centre - BRTA  
Arrasate-Mondragon, Spain  
gelezgarai@ikerlan.es

Iñigo Zubitur  
Department of Energy Storage  
and Power Electronics (BPE)  
Ikerlan Technology Research  
Centre - BRTA  
Arrasate-Mondragon, Spain  
izubitur@ikerlan.es

Itsasne Landaburu  
Department of Energy Storage  
and Power Electronics (BPE)  
Ikerlan Technology Research  
Centre - BRTA  
Arrasate-Mondragon, Spain  
ilandaburu@ikerlan.es

Mikel Lopez  
Department of AI & Data (DAI)  
Ikerlan Technology Research  
Centre - BRTA  
Arrasate-Mondragon, Spain  
mikel.lopez@ikerlan.es

Endika Bilbao  
Department of Energy Storage  
and Power Electronics (BPE)  
Ikerlan Technology Research  
Centre - BRTA  
Arrasate-Mondragon, Spain  
ebilbao@ikerlan.es

Irma Villar  
Department of Energy Storage  
and Power Electronics (BPE)  
Ikerlan Technology Research  
Centre - BRTA  
Arrasate-Mondragon, Spain  
ivillar@ikerlan.es

**Abstract**— The transition to electrification of maritime transport is crucial to mitigate greenhouse gas emissions, and the International Maritime Organisation (IMO) has set ambitious reduction of 40% of the emissions for 2030. A key element of this transition is the electrification of vessels, which requires an efficient charging infrastructure. This paper proposes a comprehensive charger model adapted to electrified and hybridised vessels, which addresses the challenges of managing the charging process and optimising port availability. Leveraging Digital Twin technology, the model integrates electrical and thermal considerations, enabling real-time monitoring and control. The charger model consists of a two-stage system: a three-phase transformer stage and an AC-DC converter stage, each of which is modelled for accurately capture the electrical behaviour and thermal dynamics. In addition, the methodologies for implementing the model on a cloud platform, facilitating remote access and management, are proposed.

**Keywords**— Power Converter, Transformer, Electric Vessel, Digital-Twin, Modeling, Cloud, AWS.

## I. INTRODUCTION

Maritime transport represents 2.5% of total greenhouse gas emissions. To overcome this issue, International Maritime Organization has established a reduction of 40% of the emissions for 2030. Therefore, the future of maritime transport is expected to be driven by the electrification of vessels. As of today, the fleet of identified electrified and hybridized ships amounts to 472 ships [1] and it is expected a grow of around 30% by 2030 [2]. In [3] the case study of a tugboat electrification is presented, where the state of the art in the actual maritime electrification scenario is explained.

In this context, the main challenge is the management of the charging process as well as the different ports availability. Therefore, it is important to monitor the chargers located in the respective ports, as well as the information of each port such as

the available energy, to estimate the charging times and optimize the process. To overcome this scenario, the use of Digital Twins is becoming more and more common, as they are able to run system models in real time and can be deployed on cloud platforms to access them from any location.

The concept of Digital Twin is gaining popularity in various industries, driven by machine learning, data mining and the Internet of Things (IoT) advances [4]. In the power electronics field, digital twins play a crucial role in predictive maintenance, real time monitoring and control, in particular in the context of DC converters. In [5] the authors have demonstrated the efficacy of real-time Digital Twins for power electronic converters through the development and experimental validation of a Digital Twin model of a DC-DC boost converter. Furthermore, the development of real-time models for power electronic converters using dynamic neural networks has been proposed in recent work [6], presenting a novel approach that combines time-domain, switch-averaged, large-signal, and embeddable characteristics. However, Digital Twin have the difficulty that they require challenging architectures and complex models that are capable of running fast to implement them in real time.

According to grid connected chargers, in the literature, numerous approaches for modelling the converters and transformers topologies are presented, especially for electric vehicle charging. Concerning the grid side transformers, a large number of different approaches have been used to model transformers electrically and thermally. In [7] various models for linear transformers in circuit simulation are discussed, including the reluctance model, inductance matrix model, T-model, and reduced T-model. A comprehensive model for multiple-winding transformers and coupled inductors is presented in [8], enabling direct measurement of all parameters for various winding geometries. Regarding the thermal modelling, to address limitations due to unbalanced operation,

in [9] authors propose a modified thermal circuit model that considers interphase thermal coupling by analysing internal heat sources, reevaluating environmental influences, and conducting temperature-rising tests to calculate interphase thermal coupling coefficients. On the other hand, a dynamic thermal model with equivalent non-linear temperature dependent thermal resistances is introduced in [10], where heat sources are determined taking into account non-sinusoidal excitations, and frequency dependent effects.

On the converter side, also many contributions of different converter topologies modelling are available in the literature. In [11] DC-DC converters modelling with capacitor Equivalent Series Resistance (ESR), focusing on operation in continuous conduction mode is proposed, performing simulations in MATLAB®/SIMULINK®.

However, the challenge of converter and transformer models for Digital Twin implementation is that they are often complex models that include semiconductor switching and slow dynamics, making real-time model implementation difficult. Therefore, in many cases it is necessary to linearise or implement averaged models that allow simulation at the same time as the real system.

In this paper, a charger model composed of two stages is proposed. The first one represents the three-phase transformer, that is modelled electrically and thermally using a combination of the average circuit model and a thermal network model. This model is able to support the grid changes as it includes a foster equivalent circuit for the different electrical parts, in order to perform a frequential model. The second part is linked with the transformer output, implementing an average AC-DC converter model that is able to run fast and represent the converter dynamics in real time, also including the temperature increase estimation, following the thermal network methodology.

This paper is structured in four sections. Section II explains the modelling of the charger, describing how each part has been modelled. In section III the simulation of the model is carried out emulating the grid and the batteries of the vessels, in order to verify the correct operation. Section IV introduces the implementation of the cloud model, defining the methodology for moving from the implemented model to an integrated cloud platform running on real time. In section V the cloud implementation that integrates the developed models is proposed. Finally, conclusions are presented in section VI.

## II. CHARGER MODELLING

The charger model proposed in this paper consists of two main stages: the three-phase transformer stage and the AC-DC converter stage. Each stage is modelled electrically and thermally to accurately represent its behaviour under various operating conditions as grid harmonics distortion and different battery charging requests.

### A. Transformer modelling

The transformer selected for this application is a three phased three-winding transformer, composed of a Delta primary, and two Wye secondary windings, around a three-limb core Fig. 1. In practical applications, the low-voltage side windings should be grounded through a resistance or reactance

to limit earth fault currents. This connection type is usually used in double secondary transformers, which means that both low-voltage windings are identical.

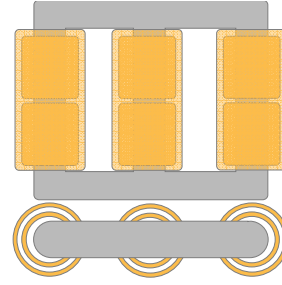


Fig. 1. Three phase transformer composed of one primary and two secondary windings.

To model the transformer, an electrical circuit model that represents the electromagnetic behaviour is used, where the different parts as leakage and magnetizing inductance and the equivalent parasitic capacitance are modelled to measure the losses in the windings and core. For obtaining the temperature increase, the electrical circuit losses are introduced into a resistance thermal network that represents the transformer heat distribution.

The electrical model of a three-phase three-winding D-Yy-Y transformer is similar to that of a single-phase three winding transformer. This single-phase three-winding transformer can be modelled as shown in Fig. 2.

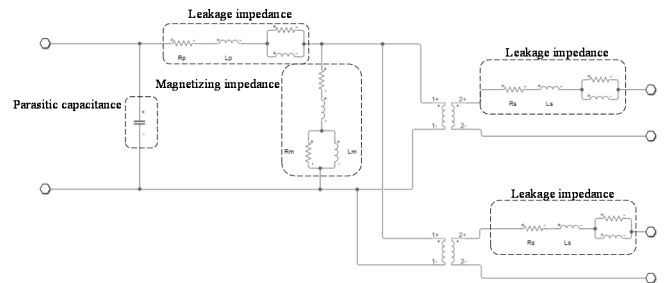


Fig. 2. Single phase three winding transformer electrical model.

The model includes the equivalent leakage impedance of the three windings, and a magnetizing branch for modelling the core losses, as well as an ideal transformation ratio. This model is reasonably accurate when the core is not saturated and is the most used in power systems studies. If a more accurate behaviour of the magnetic core is required, there are another equivalent circuit models, such as the proposed in [12] where it is possible to get very accurate results when the model is used to describe the behaviour of the magnetic core, adding the saturation curves instead of the typical nonlinear resistance model. Or the equivalent circuit proposed on [13] that take into account turn-to-turn fault conditions, facilitating computer-aided analysis across various software platforms.

Besides including all the parameters explained to adequate the single-phase model to the three-phase one, it is important to take into account the zero-sequence impedance. The equivalent circuit of this impedance depends on the type of winding connections and the core construction. The different zero

sequence impedance circuits for various winding configurations are well described in [14].

As the transformer primary winding is connected to the grid, a frequential model is implemented using the foster equivalent impedance to support the incoming harmonics [15]. This equivalent circuit is useful for analysing the frequency response of a transformer, as it allows the prediction of the transformer's behaviour under different operating conditions, such as frequency and load variations. The circuit is composed by a combination of series and parallel impedances that represents the winding resistance and leakage inductance for a low- and mid- frequency transient Fig. 3. It is important to use this approach in the model, since the harmonics coming from the grid can have a big impact and it is crucial to take them into account.

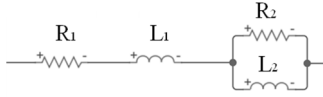


Fig. 3. Foster equivalent model for leakage and magnetizing impedances.

Finally, it is also important to include an equivalent parasitic capacitance in the input of the system, considering the winding to winding, layer to layer and the stray capacitance in order to be able to measure and detect possible resonances in the circuit.

For modelling the thermal behaviour of the transformer, a thermal resistance network is used. A thermal network is a mathematical model that represents the thermal behaviour of the transformer. The model is used to predict the temperature rise under different operating conditions, such as load and ambient temperature variations. These networks include series of thermal resistances that represents the heat transfer between the different parts of the transformer. The transformer resistance network can be divided into three main components: conduction, convection, and radiation.

The conduction resistance is divided in the air conduction resistances and the conduction resistances in a solid body. The conduction resistance in a solid body is determined by solid components, such as the windings and the core, and the thickness and area of each component. It is a function of the thermal conductivity, the density, and the distance through which heat is conducted. It is calculated using (1).

$$R_{conduction} = \frac{d}{k A} \quad (1)$$

Where  $d$  is the distance over which heat is conducted,  $k$  is the thermal conductivity of the solid, and  $A$  is the surface area.

The air conduction resistance in natural convection refers to the resistance to heat transfer that arises due to the conduction of heat through the air. The equation used for calculating this resistance is similar to the solid conduction one. Note that this equation is valid only for non-moving air conduction.

The convection resistance is determined by the coefficient of heat transfer between the transformer's surface and the surrounding air, and the area of the surface (2).

$$R_{convection} = \frac{1}{h A} \quad (2)$$

Where  $h$  is the heat transfer coefficient and  $A$  is the surface area.

The heat transfer coefficient is a function of several factors, including the temperature, density, volumetric expansion coefficient, dynamic viscosity, kinetic viscosity, and thermal conductivity.

Once the mentioned parameters are obtained for each node, the different correlations equations are applied for calculating the  $h$ . In this case, the nodes that involve convection are in laminar regime and natural convection, so the heat transfer coefficient is calculated using the Nusselt correlation equation divided in the vertical and horizontal direction.

The Nusselt number is a dimensionless number that describes the ratio of convective heat transfer to conductive heat transfer in a fluid. It can be calculated analytically, based on the Grashof number ( $Gr$ ) and the Prandtl number ( $Pr$ ). In the TABLE I, the Nusselt number analytical equations for horizontal and vertical orientations are shown.

TABLE I. NUSSULT CORRELATION EQUATION FOR HORIZONTAL AND VERTICAL DIRECTIONS.

Nu horizontal	$N_u = 0.54 (Gr, Pr)^{\frac{1}{4}}$
Nu vertical	$N_u = 0.59 (Gr, Pr)^{\frac{1}{4}}$

It is important to mention that this Nusselt approximation equation is only accurate for laminar flow regimes, it is not suitable for turbulent regimes. Additionally, this equation is based on a general assumption, and it may not be accurate for some specific cases, such as low Grashof number and high Prandtl number. Another manner for calculating this is using the Churchill-Chu correlation approach which is explained in [16].

Finally, the radiation resistance is determined by the coefficient of heat transfer between the transformer's surface and the surrounding surfaces, and the area of the surface. (3) is used for calculating this resistance.

$$R_{radiation} = \frac{1}{\sigma e A \Delta T^4} \quad (3)$$

Where  $e$  is the surface emissivity,  $\sigma$  is the Stefan-Boltzmann constant,  $A$  is the area of the surface and  $\Delta T$  represents the temperature difference.

The implemented resistance network Fig. 4 uses the described resistances for estimating the temperature increase in each defined node.

Analysing the thermal network, the core is divided in 12 sections (nodes 2, 3, 4, 5, 6, 7, 9, 11, 12, 13, 14 and 15). Then, each winding is divided in 2 parts, the inner parts (nodes 8, 10, 23, 24, 25 and 26) represents only one face of the winding while the outer parts (nodes 1, 16, 21, 22, 27 and 28) represents the rest of the contour. Finally, there are 4 vacuum points between components (nodes 17, 18, 19 and 20) where it is interesting to measure the temperature increment.

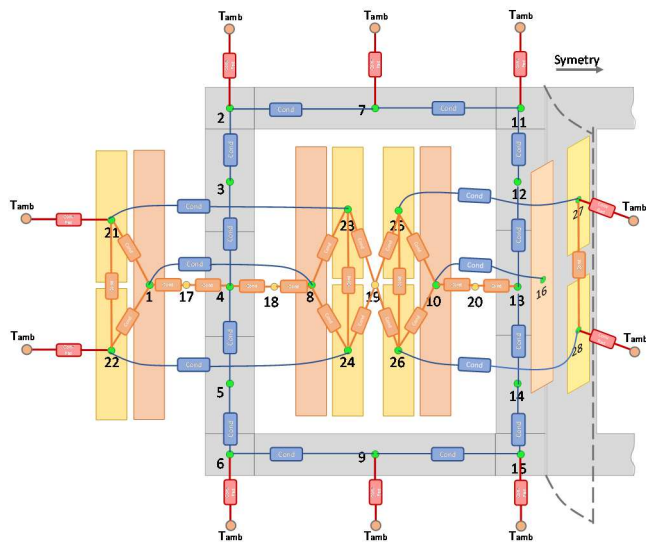


Fig. 4. Transformer thermal model representation, including the different nodes and thermal resistances.

Regarding the resistors, the hierarchy is the following: convection and radiation heat transfer in red, air conduction by natural convection in orange and conduction between two solid bodies in blue, in this case the core and the windings.

To conclude, the connection between the electrical and thermal model is done using the core and windings nodes, where the losses obtained from the electrical model are divided between the mentioned windings and core sections and inserted as a thermal energy source.

### B. Converter modelling

The topology of the converter is shown in Fig. 5. The system is composed of two series connected AC-DC inverters with a corner-ground mid-point connection. With this topology each converter blocks half of the output voltage allowing the use of lower voltage rating semiconductors, reducing the overall cost of the topology.

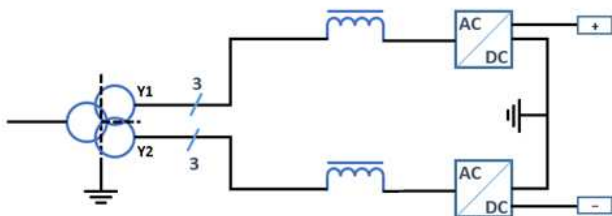


Fig. 5. AC-DC inverter representation.

By grounding the middle point of the bus, a bipolar distribution is achieved, which has several advantages over unipolar distribution [17]. The insulation voltage rating required for the cables is reduced, low-power loads can be connected between pole to ground (i.e., across 500 V or 750 V terminal) and the high-power loads can be connected across the pole to pole (corresponding to 1000 V or 1500 V typical battery voltage). Moreover, a bipolar DC bus architecture is more reliable than the unipolar system as it can operate with only one

DC bus (positive or negative) in case of a fault. This is typically used in Aircraft and marine vessel power distribution.

However, a bipolar topology has an inherent voltage imbalance issue on the positive and negative DC buses due to stochastic load consumption occurrences and their different load characteristic. The aforementioned unbalancing issue can be addressed by employing bipolar DC converter topologies or multilevel converters with neutral point-or independent converters per semi-bus. Having in mind that 500 V to 750 V semi-bus voltage is a typical industrial voltage level, using an independent converter per semi-bus makes use of widely available commercial power blocks. This also splits the total power between two converters. Therefore, gathering this benefits a solution with a three-phase 2-level converter per semi-bus is preferred.

The developed converter model is composed of two domains, the electrical domain in which no power losses are calculated and the thermal domain where the power losses are calculated to estimate the inverter inner temperature. The thermal model is dependant of the electric one, as the data collected from this last domain is used to calculate the inverter losses.

In order to have a fast model capable of following the real system dynamics, some simplifications are assumed. The electric model does not take into account the losses and it is considered as an ideal inverter, and the two inverters are treated as identical. With those assumptions, the thermal model can be simplified to one inverter.

On the one hand, the electrical model is a no current control loop average model, no commutations are simulated and the synchronization between the grid and converter is achieved by equations, considerably reducing the simulation time. This model receives as an input the voltage provided by the battery and the constant current and voltage values set by the operator with which the converter performs a typical charge profile. The converter operates at both constant current (CC) and constant voltage (CV) charging mode. First, in the CC charge, the battery is charged with a specified constant current until reaches a pre-set voltage level. Then the CV charge begins, where constant voltage is applied to the battery, and in consequence, the current reduces as the battery becomes fully charged.

The thermal model is based on Cauer thermal network Fig. 10. The first node represents the junction of one of the semiconductors of and it is connected to the heatsink node by thermal resistances. In the heatsink node the rest of the converters switch nodes are gathered and a convective connection with the ambient is done.

The heat source of each switch is calculated by analytical equations. These equations are a fast and accurate mode of estimating the temperature increase, as they are based on values obtained from the switches' datasheets.

### III. MODEL IMPLEMENTATION ON MATLAB<sup>®</sup>/SIMULINK<sup>®</sup>

The transformer and converter models described in the previous section are integrated in MATLAB<sup>®</sup>/SIMULINK<sup>®</sup> using Simscape library, which enables the use of both electrical and thermal components.

In TABLE II, the main parameters of the model are shown.

TABLE II. CHARGER MAIN PARAMETER VALUES.

Grid voltage	400V
Grid frequency	50Hz
Transformer secondary voltage	22kV
Battery voltage	777V
Switching frequency	8kHz
Ambient temperature	25°C

For the model validation in SIMULINK®, an ideal battery model is used to emulate the charging process of the real system battery. This approach will represent the charge and discharge profile of the real system battery. For the grid, considering that the final model will have the harmonics and amplitude data coming from the grid measurements, a three-phase signal generator is implemented, which reconstructs the grid signals based on the amplitudes-frequencies of the harmonics Fig. 10.

The transformer electrical model is implemented in SIMULINK® as shown in Fig. 6, where the different foster impedances are used to model the leakage inductance and the magnetizing inductance branches. Then, the transformation relation is implemented using an ideal linear transformer, as the losses in the windings are estimated in the leakage impedance branches.

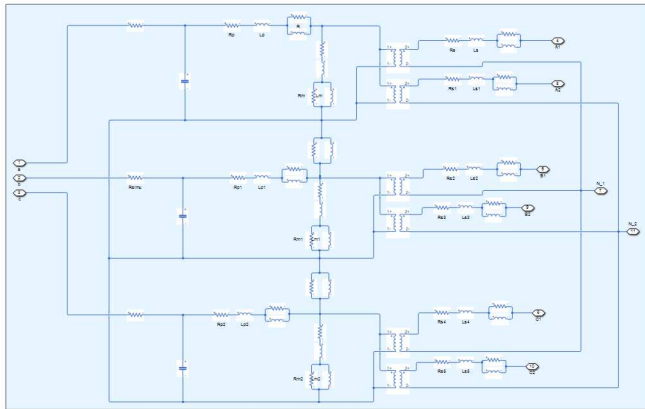


Fig. 6. Transformer electrical model subsystem.

To implement the thermal model, the resistor network is built using the thermal blocks of Simscape. The values of the conduction, convection and radiation resistances are calculated using a MATLAB® script included in the model and the calculated values are inserted in each resistance block Fig. 7.

Then, the power losses coming from the electrical model are divided into the different thermal nodes. These nodes include a heat source where the calculated power losses are introduced for obtaining the temperature increase in each node. With that it is possible to visualize the temperature increase in each node and to calculate the average temperature in the windings and core of the transformer.

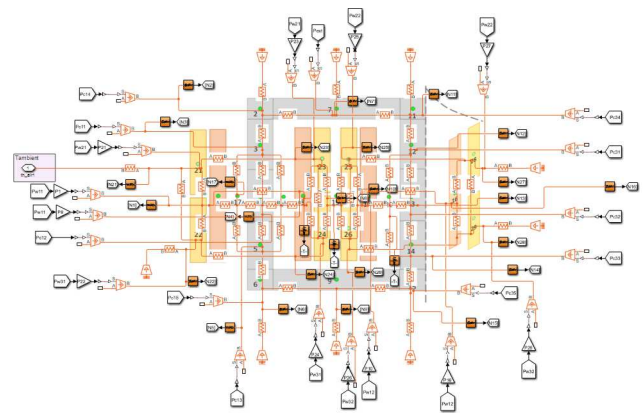


Fig. 7. Transformer thermal model subsystem.

As mentioned in section II.B, several simplifications are applied to obtain a converter fast model. As a result, an average model is implemented, where the electrical domain the commutated switches are replaced by averaged semiconductors Fig. 8.

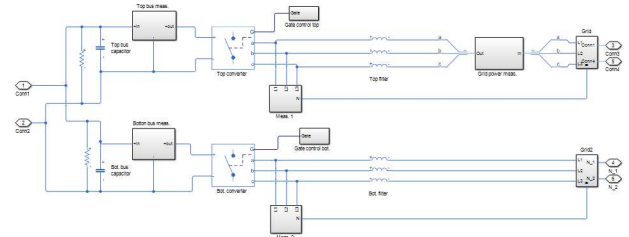


Fig. 8. Converter average model subsystem.

In the thermal domain, analytical equations are included to calculate the power losses. These equations takes the converter electrical model voltages and currents and estimates analytically the power losses in the semiconductors. Then, as in the transformer model, the calculated losses are introduced in the converter thermal model where the different conductive and convective heat transfer is modelled following the above mentioned Cauer approximation Fig. 9.

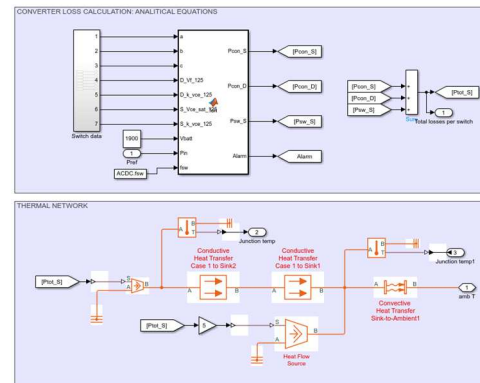


Fig. 9. Converter thermal model subsystem.

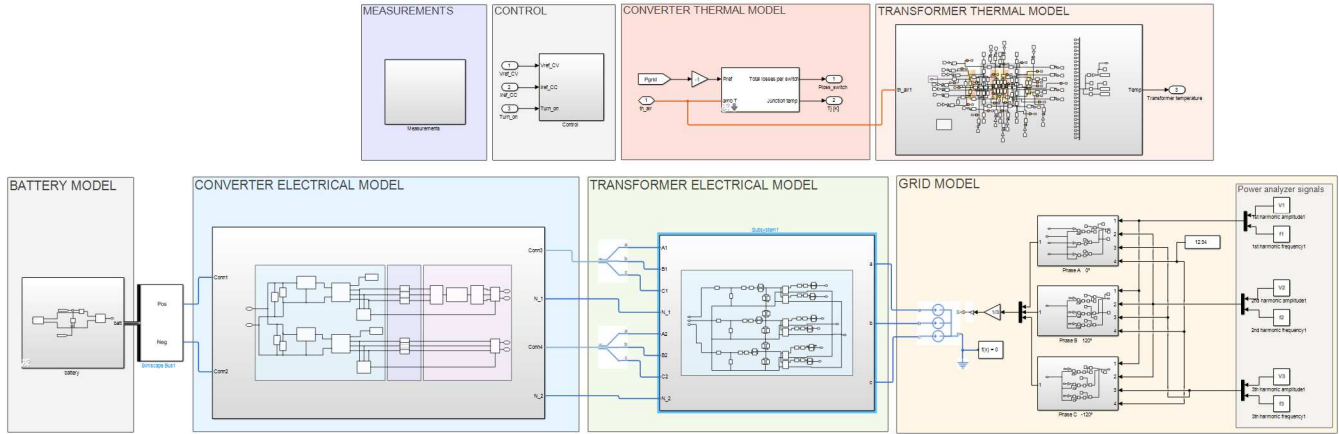
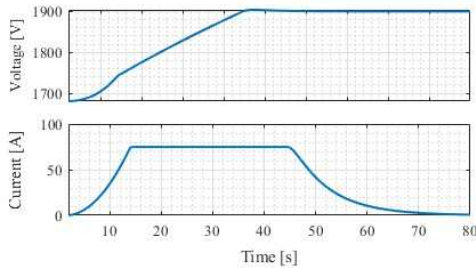


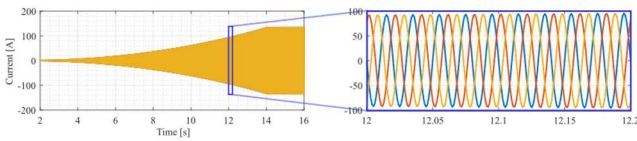
Fig. 10. Full charger model simulation on SIMULINK®.

#### IV. SIMULATION RESULTS

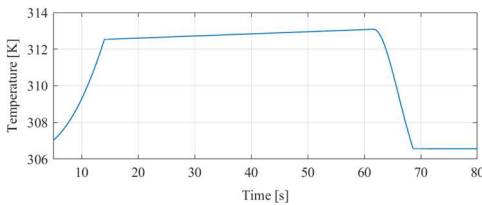
Finally, the developed charger model is tested with real system charging profile to perform a unit testing. From one side, the converter waveforms are shown in Fig. 11. It can be seen how the charging profile, where the battery is charged with 75A constant current until it reaches the desired voltage and then constant voltage charge begins. This profile requires a current consumption coming from the transformer output, that is incremented until constant current is reached.



a) Battery voltage and current waveforms during charging.



b) Converter input current waveforms at the beginning of the charging.



c) Converter switches junction temperature.

Fig. 11. Charger model simulation waveforms.

On the other side, the transformer input voltage coming from the grid is shown in Fig. 12. where it can be observed the grid distortion due to the impact of 3<sup>rd</sup> and 5<sup>th</sup> harmonics. These harmonics are introduced in the frequential model of the windings, where the transformer losses are calculated and introduced into the thermal model.

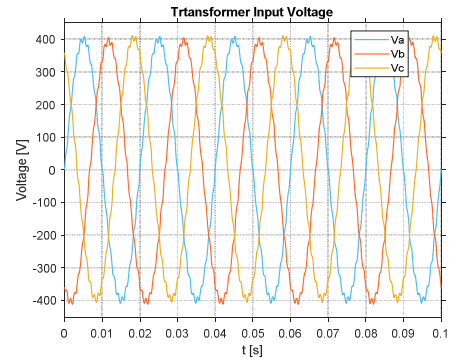


Fig. 12. Transformer input voltage waveforms.

#### V. CLOUD REAL TIME IMPLEMENTATION

After the study of the different platforms and cloud service providers such as Azure, AWS, Google Cloud and OVH, AWS is chosen because it provides services such as IoTCore required for data exchange and S3 as storage to define the DataLake.

The IoT Core service will be used to exchange the data captured by the sensors of vessels, chargers, and power grid. This service enables support for multiple protocols such as MQTT (Message Queuing Telemetry Transport) and HTTP (Hypertext Transfer Protocol) allowing devices to interoperate with the platform. It also offers high scalability and security by providing multiple layers of security to protect data. But one of the advantages of this service is that rules and customized actions can be set, allowing to the possibility to indicate where this data will be stored. In this case the captured data will be stored in a DataLake using the AWS S3 service for its definition. The core of this solution is based on two Elastic Compute Cloud

(EC2) instances which provide scalable computing capacity on demand.

A block diagram that represents the cloud solution architecture based on two EC2 is shown in Fig. 13.

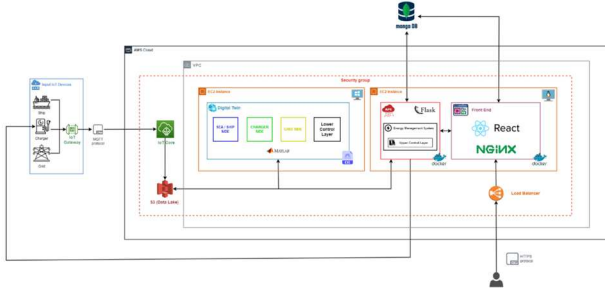


Fig. 13. Cloud solution diagram, where the two EC2 instances are shown.

On the one hand, the instance EC2 containing the Digital Twin model will be T2.Large based on Windows. With that, it is possible to install the MATLAB<sup>®</sup> Runtime that allows to launch the executable which contains the charger model. In order to run the Digital Twin executable on the Windows-based EC2 instance, an Application Programming Interface (API) has been developed and deployed using the Flask framework on this instance. This API features two endpoints, enabling the initiation of a loop executing the executable and facilitating on-demand termination. The outputs generated by the Digital Twin are stored in a dedicated DataLake and a MongoDB database. On the other hand, the other instance EC2 will be T2.Micro based in Ubuntu. Here the charger model that predicts the charging and a front end that will monitor the different charging processes are placed. Both services will be dockerized to facilitate the implementation.

This cloud implementation sets the integration of an advanced Energy Management Strategy (EMS) and a Digital Twin that can operate in real-time on a single, unified platform. This platform offers the flexibility to accommodate diverse source codes, allowing them to run seamlessly alongside each other.

## VI. CONCLUSIONS

An electrical and thermal modelling of an electric vessel charger was developed, using linearized and average models. These models can be implemented on MATLAB<sup>®</sup>/SIMULINK<sup>®</sup> in order to perform real-time simulations and integrate them on a cloud-based platform. The developed models demonstrate the importance of implementing averaged models in order to be able to implement real-time application, validated in simulations. Furthermore, a cloud solution is proposed for a Digital Twin implementation. This solution allows the direct implementation of previously developed models, reducing timing and facilitating the correlation between the simulations and real application. This solution will be part of a final development in a real implementation of an electric vessel multi-MW recharging.

## ACKNOWLEDGMENT

This research was developed under European Horizon Europe Framework Programme (HORIZON) under grant agreement No. 101056853 within the HYPOBATT Project (Hyper Powered Vessel Battery Charging System).

## REFERENCES

- [1] "DNV Alternative Fuel Insight platform," DNV - Maritime Battery Forum, [Online]. Available: <http://afi.dnvgl.com>. J. Clerk Maxwell, A Treatise on Electricity and Magnetism, 3rd ed., vol. 2. Oxford: Clarendon, 1892, pp.68–73.
- [2] "World Fleet Register," Clarksons, [Online]. Available: <https://www.clarksons.net/wfr/>.
- [3] M. Hayton (2023). Marine Electrification is the Future: A Tugboat Case Study. In: Y. Li, Y. Hu, P. Rigo, F.E. Lefler, G. Zhao. (eds) Proceedings of PIANC Smart Rivers 2022
- [4] A. Rasheed, O. San and T. Kvamsdal, "Digital Twin: Values, Challenges and Enablers From a Modeling Perspective," in IEEE Access, vol. 8, pp. 21980-22012.
- [5] K. Sado, J. Hannum and K. Booth, "Digital Twin Modeling of Power Electronic Converters," 2023 IEEE Electric Ship Technologies Symposium (ESTS), Alexandria, VA, USA, 2023
- [6] A. Wunderlich and E. Santi, "Digital Twin Models of Power Electronic Converters Using Dynamic Neural Networks," 2021 IEEE Applied Power Electronics Conference and Exposition (APEC), Phoenix, AZ, USA, 2021
- [7] Q. Chen, F. C. Lee, J.Z. Jiang and M. M. Jovanovic, "A new model for multiple-winding transformer," Proceedings of 1994 Power Electronics Specialist Conference - PESC'94, Taipei, Taiwan, 1994
- [8] G. W. Ludwig and S.-A. El-Hamamsy, "Coupled inductance and reluctance models of magnetic components," in IEEE Transactions on Power Electronics, vol. 6, no. 2, pp. 240-250, April 1991
- [9] Y. Ding et al., "Modified thermal circuit model for distribution transformers in three-phase unbalanced operation," 2017 1st International Conference on Electrical Materials and Power Equipment (ICEMPE), Xi'an, China, 2017
- [10] I. Villar, U. Viscarret, I. Etxeberria-Otadui and A. Rufer, "Transient thermal model of a medium frequency power transformer," 2008 34th Annual Conference of IEEE Industrial Electronics, Orlando, FL, USA, 2008
- [11] P. Špánik, M. Frivaldský and P. Drgoňa, "Optimization procedure for selection of active components of DC-DC converter's thermal simulation model," 2014 ELEKTRO, Rajecké Teplice, Slovakia, 2014
- [12] J. A. Martinez, "Parameter Determination for Power Systems Transients," 2007 IEEE Power Engineering Society General Meeting, Tampa, FL, USA, 2007
- [13] M. Gholami, E. Hajipour and M. Vakilian, "A single phase transformer equivalent circuit for accurate turn to turn fault modeling," 2016 24th Iranian Conference on Electrical Engineering (ICEE), Shiraz, Iran, 2016, pp. 592-597
- [14] J. S. Song, et al. "Determination method for zero-sequence impedance of 3-limb core transformer." (2019).
- [15] F. de Leon and A. Semlyen, "Time domain modeling of eddy current effects for transformer transients," in IEEE Transactions on Power Delivery, vol. 8, no. 1, pp. 271-280, Jan. 1993
- [16] S.W. Churchill and H.H. Chu, "Correlating Equations for Laminar and Turbulent Free Convection from a Horizontal Circular Cylinder," International Journal of Heat and Mass Transfer, vol. 17, pp. 1323-1329, 1974
- [17] S. Rivera, R. Fuentes, S. Kouro, T. Dragicevic and B. Wu, "Bipolar DC Power Conversion: State-of-the-Art and Emerging Technologies," IEEE Journal of Emerging and Selected Topics in Power Electronics, pp. 1-1, 2020